Coherent Structures in Jet Turbulence and Noise

Ralph R. Armstrong* and Alfons Michalke†
Technische Universität, Berlin, Germany
and
Helmut V. Fuchs‡
Deutsche Forschungs- und Versuchsanstalt für Luft- und Raumfahrt, Berlin, Germany

Experimental results of pressure cross-spectra in model jets indicate that large-scale coherent structures do persist at higher Mach numbers up to 0.8 in the relevant range of Strouhal numbers between 0.1 and 2.0. If the pressure field is Fourier-analyzed circumferentially, the lower-order components are seen to dominate. This, along with the high acoustic efficiency of these components, suggests a numerical calculation procedure for the radiated far-field, which is based on Lighthill's wave equation approach with a linearized pressure source function, strongly weighted by axial and radial interference functions.

Nomenclature

a_0 = speed of sound
C_ω = coincidence spectral density function
D = jet nozzle diameter
f = frequency
$\tilde{F}_{r,m}$ = radial interference function
$\tilde{F}_x$ = axial interference function
He = D/λ, Helmholtz number
J_m = Bessel functions of first kind and order m
L_p = $20 \log \tilde{p}/p_0$, equivalent sound pressure level
M = U_0/a_0, Mach number
p = turbulent jet pressure
p_0 = $20\ \mu N/m^2$, reference sound pressure
$\tilde{p}$ = root-mean-square pressure
$\tilde{p}^2_\omega$ = power spectral density of pressure
Q_ω = quadrature spectral density function
r = distance from jet axis
$\bar{r}$ = distance from center of jet exit
R = r/D
$\tilde{R}$ = $\bar{r}/D$
Re = $U_0 D/\nu$, Reynolds number
S_ω = $(C^2_\omega + Q^2_\omega)^{1/2}$
St = fD/U_0, Strouhal number
$\bar{u}$ = mean axial velocity component
U = $\bar{u}/U_0$
U_0 = jet exit velocity
$\bar{v}$ = mean radial velocity component
V = $\bar{v}/U_0$
W_{MT} = power spectral density of radiated pressure due to mean-flow/turbulence interactions
$W_{p1\,p2}$ = cross-spectral density of jet pressure
$\tilde{W}_{12,m}$ = azimuthal constituents of $W_{p1\,p2}$
x = axial coordinate along jet axis
X = x/D
Δ = difference sign
Θ = far-field angle to jet axis
λ = acoustic wavelength
ν = kinematic viscosity
ρ_0 = mean fluid density at center of jet exit
ϕ = azimuthal angle
ψ_ω = phase angle of $W_{p1\,p2}$
$\psi_{\omega,m}$ = phase angle of $\tilde{W}_{12,m}$
ω = angular frequency

Presented as Paper 76-490 at the AIAA 3rd Aero-Acoustic Conference, Palo Alto, Calif., July 20-23, 1976; submitted Aug. 12, 1976; revision received April 20, 1977.
Index categories: Nonsteady Aerodynamic; Noise.

*Research Assistant, Hermann-Föttinger-Institut für Thermo- und Fluiddynamik.
†Professor, Herman-Föttinger-Institut für Thermo- und Fluiddynamik.
‡Scientist, Institut für Turbulenzforschung.

Introduction

OUR understanding of how noise is generated by the turbulent mixing of a round jet with the surrounding medium has been enhanced since orderly structures were identified by several techniques. The large-scale phenomena show up most clearly in the fluctuating jet pressure field induced by the mixing process. The idea of large-scale coherent sound source patterns inside turbulent jets now is supported by a growing number of researchers, as may be inferred from published accounts[1-3] of the 1970 Symposium on Aerodynamic Noise (University of Loughborough), the 1973 AGARD Meeting on Noise Mechanisms (Brussels), and the 1974 Colloquium on Coherent Structures in Turbulence (University of Southampton).

If coherent turbulence structures actively take part in the jet noise generation process, it is essential that the theoretical treatment of this problem account for the acoustic interference of sound waves emanating from different parts of the jet. An appropriate procedure, favored by the joint DFVLR and TUB group, was proposed by Michalke[4] and Michalke and Fuchs.[5] The theory is based on Lighthill's acoustic analogy approach and, in its present state of development, concentrates on the mean-flow/turbulence interactions, which generally are accepted as the dominant contributors to subsonic jet noise at small angles Θ to the jet

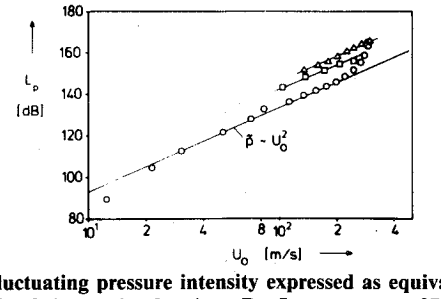

Fig. 1 Fluctuating pressure intensity expressed as equivalent sound pressure level in a circular jet: $D=5$ cm; □ $x=3D$, $r=0.5D$; ○ $x=2D$, $r=0$; △ $x=2D$, $r=0$ (nozzle with 5 mm tab).

axis. The analysis can be extended to account for gradients in the temperature field. The main advantage of this approach is that only the cross-spectral density of the turbulent jet pressure $W_{p_1p_2}$ has to be evaluated over the entire jet and not the Reynolds stress tensor.

The present paper reports on measurements of the azimuthal constituents $\tilde{W}_{12,m}$ of the pressure cross-spectral density function $W_{p_1p_2}$. The measuring technique was discussed previously, and results at low Mach number were published by Fuchs.[6] One major result concerns the effect of Mach number on the structure of the turbulent pressure field. The experiments were done for $10^4 \leq Re \leq 10^6$ and $0.1 \leq M \leq 0.7$. Narrowband analyses were confined to $0.1 \leq St \leq 2.0$.

Review of the Theory

In the theory described by Michalke and Fuchs,[5] cylindrical coordinates X, R, and ϕ are introduced inside the source region. Because of natural symmetry in an axisymmetric jet, any turbulent quantity may be expanded into a Fourier series with respect to ϕ. Additional symmetry conditions apply to the cross-spectral density of the turbulent pressure fluctuations,

$$W_{p_1p_2} = W_{p_1p_2}(X_1, R_1, X_2, R_2, \Delta\phi) \tag{1}$$

in the sense that $W_{p_1p_2}$ depends on $\Delta\phi = \phi_2 - \phi_1$, rather than on ϕ_1 and ϕ_2 individually, and that $W_{p_1p_2}$ is a symmetric function with respect to $\Delta\phi$. Under these circumstances the complex cross-spectral density can be expanded into the following Fourier series:

$$W_{p_1p_2} = \sum_{m=0}^{\infty} \tilde{W}_{12,m}(X_1, R_1, X_2, R_2) \cos m\Delta\phi \tag{2}$$

The far-field power spectral density of the noise produced by mean-flow/turbulence (MT) interactions then may be compactly written as

$$W_{MT}(\tilde{R}, \theta) = \frac{1}{\tilde{R}^2} \sum_{m=0}^{\infty} \int_V \mathrm{d}\tilde{V}_{a1} \int_V \mathrm{d}\tilde{V}_{a2}\, \tilde{W}_{12,m} \tilde{F}_{r,m} \tilde{F}_x \tag{3}$$

where the integration with respect to ϕ_1 and ϕ_2 already has been performed (see Ref. 5). Therefore, the integration in Eq. (3) is over annular volume elements given by

$$\mathrm{d}\tilde{V}_{a_1} = \mathrm{d}V_{a_1}/D^3 = 2\pi R_1 \mathrm{d}R_1 \mathrm{d}X_1$$

$$\mathrm{d}\tilde{V}_{a_2} = 2\pi R_2 \mathrm{d}R_2 \mathrm{d}X_2 \tag{4}$$

The source integral, Eq. (3), incorporates weighting functions $\tilde{F}_{r,m}$ and $\tilde{F}_x$. The latter may be termed "axial interference function," since it is of the form

$$\tilde{F}_x = \exp(-i\tau) \tag{5}$$

with an axial displacement variable of

$$\tau = 2\pi St\, M(X_2 - X_1)\cos\theta = 2\pi He(X_2 - X_1)\cos\theta \tag{6}$$

The real and imaginary parts of $\tilde{F}_x$ oscillate with $2\pi(x_2 - x_1)\cos\Theta/\lambda$ with zero crossings at multiples of π. This interference effect would be absent for vanishing Helmholtz number $He = St\,M \ll 1$ or at exactly $\Theta = 90$ deg to the jet axis.

The second weighting function in Eq. (3) is

$$\tilde{F}_{r,m} = \tfrac{1}{4} St^2 M^4 \tilde{Z}_{m,1} Z_{m,2} \tag{7}$$

where $\tilde{Z}_m$ denotes the complex conjugate of Z_m, which is given by

$$Z_m = (-i)^m \pi \{2A_0 J_m(\sigma) + i A_1 [J_{m-1}(\sigma) - J_{m+1}(\sigma)]$$

$$- A_2 [J_{m-2}(\sigma) + J_{m+2}(\sigma)]\} \tag{8}$$

The Bessel functions J_m of the first kind and order m are functions of the radial argument

$$\sigma = 2\pi St\, M\, R \sin\theta = 2\pi He\, R \sin\theta \tag{9}$$

The resulting cancellation effects, which in this case depend on $(r/\lambda)\sin\Theta$ and the respective number m, suggest the term "radial interference function" for $\tilde{F}_{r,m}$.

The complex quantities A_0, A_1, and A_2 in Eq. (8), which depend on the mean flow characteristics and the radiation

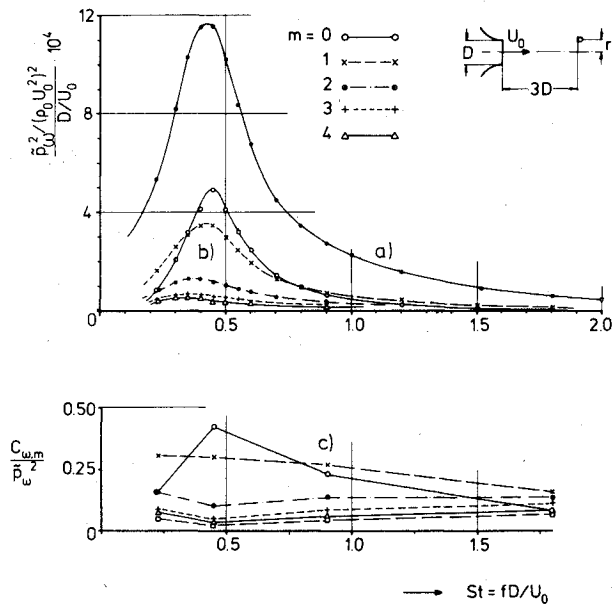

Fig. 2 Normalized power spectral densities of fluctuating jet pressure: $D = 10$ cm; $M = 0.17$; $x = 3D$, $r = 0.5D$; a) pressure as measured directly; b) azimuthal constituents of pressure as deduced from circumferential correlations; c) percentage of energy contained in individual constituents.

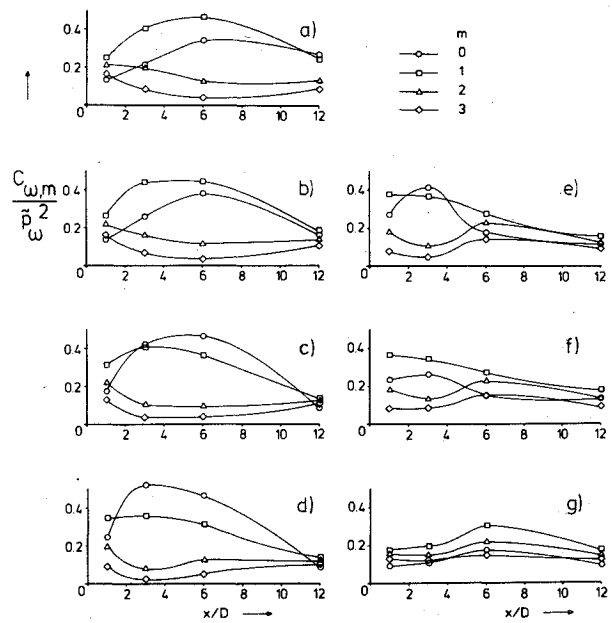

Fig. 3 Downstream development of lower-order azimuthal constituents of pressure in outer mixing region: $D = 5$ cm; $M = 0.3$; $r = 0.5D + x/6$; a) $St = 0.175$; b) 0.225; c) 0.35; d) 0.45; e) 0.7; f) 0.9; g) 1.8.

angle, are given by[5]

$$A_0 = \frac{1}{(1-UM\cos\theta)^3}\left[2\cos^2\theta\frac{\partial U}{\partial X} + \sin^2\theta\left(\frac{\partial V}{\partial R}+\frac{V}{R}\right)\right]$$

$$-i\,2\pi\,He\cos\theta\frac{(2-UM\cos\theta)}{(1-UM\cos\theta)^2}U$$

$$A_1 = \frac{\sin 2\theta}{(1-UM\cos\theta)^3}\left[\frac{\partial U}{\partial R}+\frac{\partial V}{\partial X}\right]$$

$$-i\,2\pi He\sin\theta\frac{(2-UM\cos\theta)}{(1-UM\cos\theta)^2}V$$

$$A_2 = \frac{\sin^2\theta}{(1-UM\cos\theta)^3}\left[\frac{\partial V}{\partial R}-\frac{V}{R}\right] \qquad (10)$$

in such a way that $\tilde{F}_{r,m}$ vanishes outside the flow region. Thus, $\tilde{F}_{r,m}$ limits the volume over which the source integral [Eq. (3)] is to be integrated.

With A_0, A_1, and A_2 assumed known, the essential source quantity to be measured is $\tilde{W}_{12,m}$. It is common to express the complex cross-spectral density function of the pressure in terms of real functions C_ω and Q_ω, or S_ω and ψ_ω, which can be measured directly, i.e.,

$$W_{p_1p_2} = \tfrac{1}{2}(C_\omega + iQ_\omega) = \tfrac{1}{2}S_\omega \exp i\psi_\omega \qquad (11)$$

Equation (2) then yields

$$\tilde{W}_{12,m} = \tfrac{1}{2}(C_{\omega,m} + iQ_{\omega,m}) = \tfrac{1}{2}S_{\omega,m}\exp i\psi_{\omega,m} \qquad (12)$$

where the azimuthal constituents $C_{\omega,m}$ and $Q_{\omega,m}$ or, alternatively, $S_{\omega,m}$ and $\psi_{\omega,m}$, are measured statistical averages for a pair of axial and radial coordinates X_1, R_1 and X_2, R_2.

For a small-scale random turbulence structure with thousands of statistically independent eddies, $S_{\omega,m}$ would decay rapidly with displacements ΔX and ΔR in such a way that $\tilde{F}_x$ and $\tilde{F}_{r,m}$ would hardly vary within a source correlation volume. For a large-scale coherent turbulence structure, on the other hand, variations in $\tilde{F}_x$ and $\tilde{F}_{r,m}$ may be expected to play an important role. Therefore, the determination of $C_{\omega,m}$ and $Q_{\omega,m}$ will demonstrate exactly how important acoustic interference effects are in a quantitative calculation of the far-field spectrum W_{MT} with Eq. (3).

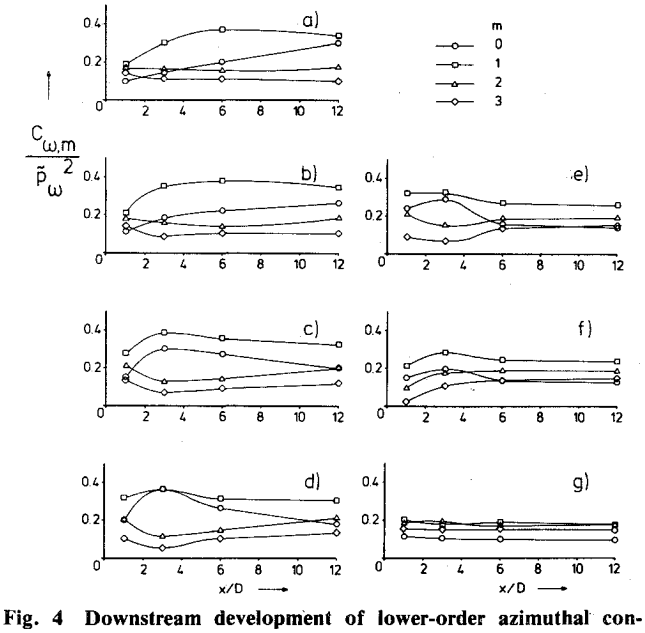

Fig. 4 Downstream development of lower-order azimuthal constituents of pressure in central mixing region: $D=5$ cm; $M=0.7$; $r=0.5D$; St, see legend of Fig. 3.

Measuring Procedure

Several different model jet rigs were used during the course of this work. The characteristics of the pressure field did not change from one jet to the other, except for measuring positions close to the nozzle exit, say at $X<1$. Although different microphone probes were tried, most of the measurements were made with standard Brüel & Kjaer 1/8-in. condenser microphones fitted with nose cones. For probe diameters far less than 10% of that of the jet ($D=10$ or 5 cm), the size of the probe had no dramatic effect on the results.

The model jet rig used here has a standard circular nozzle with an inner contour of constant curvature ($r=D$) and a cylindrical end-section 0.2 D in length. The contraction ratio was very large (100 to 400, depending on whether the 10-cm or 5-cm-diam nozzle was used). For details of the test setup and instrumentation, the reader may refer to Fuchs,[7] Fig. 1b.

The analog narrowband correlation technique recently was abandoned and replaced by a computer program. This enables us to completely analyze the pressure signals on a Hewlett Packard 2116 C digital computer.

For this purpose, the output signals of the B&K 2607 measuring amplifiers provide the 10-V peak-to-peak levels required for the low-pass filters Telco TAF 5002. The filters, which have a 48 dB/octave slope, are set to an upper limiting frequency $f_0 = St_0 U_0/D$ at a typical value of 3.2 for St_0. The two filtered signals then are digitized by two independent 12-bit home-made analog digital converters; 1193 segments of twice the 512 data words can be stored continuously on a disk for later processing of 128 spectral components of one cross- and two power-spectra. The averaging error involved in the calculated coherence can be estimated as $1/(2\cdot 1193)^{1/2} = 0.02$.

When a sampling or measuring time of 27 sec is chosen for a jet Mach number of $M=0.5$, the computing time for one set of spectra amounts to a quarter of an hour. The subsequent

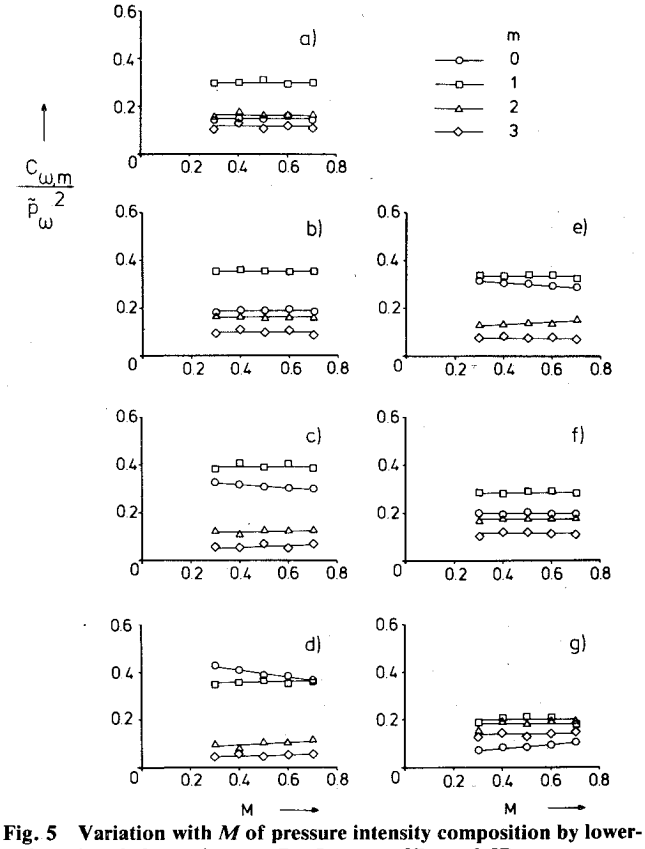

Fig. 5 Variation with M of pressure intensity composition by lower-order azimuthal constituents: $D=5$ cm; $x=3D$, $r=0.5D$.

decomposition of the circumferential correlations into $m=16$ azimuthal constituents takes only a negligible fraction of the total time required on the computer.

Characteristics of Subsonic Jet Pressure Field

Figure 1 exhibits equivalent sound pressure levels L_p at two locations in the jet as a function of U_0. The measuring position $X=3$, $R=0.5$ is where the pressure intensity is a maximum, and this position will be something like a characteristic reference point for the investigations to follow.

The results in the middle of the so-called potential core ($X=2$, $R=0$) indicate that for $U_0>250$ m/s the pressure $\tilde{p}$ increases more rapidly than U_0^2. This agrees with an earlier result by Lau (Ref. 8, Fig. 23). This phenomenon is coupled with the occurrence of standing waves within the core region as soon as the probe or some other obstacle is inserted there. This does not occur for M up to 0.8 when the probe is in the mixing region. Interactions of this kind between a probe and the flow might also be responsible for the strong sound radiation observed by other investigators when they tried to correlate the far-field pressure with the signal of a probe placed in a high subsonic Mach number jet. The standing waves disappeared in our jet when a tab similar to those investigated by Bradbury and Khadem[9] was built into the nozzle exit. Note that in the latter case (the upper curve in Fig. 1) L_p was increased by more than 10 dB in the core over the whole range of velocities.

We should note that, in the case where no tabs were used these anomalies did not exist when the microphone was positioned in the mixing region, where the center of the turbulent sound sources is assumed to lie and where, subsequently, most of our high Mach number experiments were done. The corresponding square symbols in Fig. 1 show L_p between 140 and 160 dB for $0.25<M<0.8$. These extremely high near-field pressure levels in a jet which, of course, does not radiate sound of that order, also were one of the reasons why the 1/8-in. microphone was employed here.

The power spectral density of the turbulent pressure $\tilde{p}_\omega^2$ was suitably normalized as

$$\frac{\tilde{p}_\omega^2/(\rho_0 U_0^2)^2}{D/U_0}=\frac{\tilde{p}^2(St)/(\rho_0 U_0^2)^2}{\Delta f\, D/U_0} \tag{13}$$

A typical example from Ref. 5 is reproduced here as the uppermost solid curve in Fig. 2.

In addition to the more or less standard analysis of the pressure described previously, we require an expansion or decomposition of each pressure frequency component $\tilde{p}_\omega(St)$ in a series of discrete azimuthal constituents $\tilde{p}_{\omega,m}(St)$. This may be achieved via circumferential correlations on constant radii $R_1=R_2=R$ in planes normal to the jet axis $X_1=X_2=X$, i.e.,

$$C_\omega(X,R,\Delta\phi)=\sum_{m=0}^{\infty} C_{\omega,m}(X,R)\cos m\Delta\phi \tag{14}$$

Since in this very special case the corresponding

$$Q_\omega(X,R,\Delta\phi)=\sum_{m=0}^{\infty} Q_{\omega,m}(X,R)\cos m\Delta\phi \tag{15}$$

is identically zero (because of the symmetry of our clean model jet described earlier, i.e., no swirl—no preferred circumferential direction), now we may write

$$C_\omega(\Delta\phi=0)=\sum_{m=0}^{\infty} C_{\omega,m}\equiv\tilde{p}_\omega^2=\sum_{m=0}^{\infty}\tilde{p}_{\omega,m}^2 \tag{16}$$

and hence

$$\frac{C_{\omega,m}}{\tilde{p}_\omega^2}=\frac{\tilde{p}_{\omega,m}^2}{\tilde{p}_\omega^2}=\frac{\tilde{p}_m^2(f)/\Delta f}{\tilde{p}^2(f)/\Delta f} \tag{17}$$

Thus we may obtain the m constituents of the normalized power spectral density of the pressure at a position X, R, viz.,

$$\frac{\tilde{p}_{\omega,m}^2/(\rho_0 U_0^2)^2}{D/U_0}=\frac{C_{\omega,m}}{\tilde{p}_\omega^2}\,\frac{\tilde{p}^2(St)/(\rho_0 U_0^2)^2}{\Delta f\, D/U_0} \tag{18}$$

As a result of the Fourier analysis of a circumferential correlation curve, $C_{\omega,m}/\tilde{p}_\omega^2$ henceforth may be interpreted as that fraction of fluctuating energy which is contained in any individual azimuthal constituent m of the pressure at X, R.

Figure 2 shows the three quantities coupled by Eq. (18) as measured at $X=3$ and $R=0.5$. The striking dominance of the low-order constituents $m=0$, 1, 2, 3 was the main experimental result of Ref. 5. It justifies the evaluation for only a total of $m=16$ constituents, and simplifies in many ways our further analyses of jet turbulence and noise.

Additional circumferential correlations at other radial and axial positions in the jet have reinforced these earlier results. Figure 3, for example, shows a set of data for radii $R=0.5+X/6$, i.e., along the outer boundary of the mixing region. For $St=0.45$ and $X=3$, for instance, less than 3% of $\tilde{p}_\omega^2$ is contained in modes with $m>3$.

It has been possible only recently, however, for us to compare these low Mach number results with data obtained at $M=0.7$ and thereby to extend our earlier statements.

Effect of Mach Number on Pressure Structure

After identifying the previously mentioned error inherent in probe measurements at local Mach numbers exceeding 0.6 or

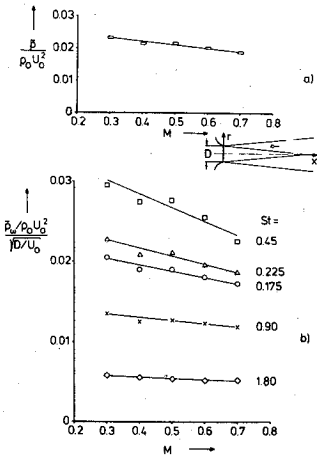

Fig. 6 Variation with M of unresolved normalized pressure intensity: $D=5$ cm; $x=3D$, $r=0.5D$; a) overall pressure, b) narrowband pressure.

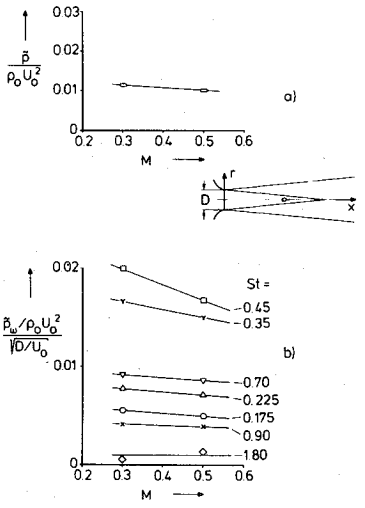

Fig. 7 Variation with M of unresolved normalized pressure intensity: $D=5$ cm; $x=3D$, $r=0$; a) overall pressure, b) narrowband pressure.

0.7, the effect of M on the pressure field was studied chiefly in the mixing region at $R=0.5$, where the local velocity is only 0.65 times that in the core region.

The data of Fig. 4 thus were obtained for $M=0.7$. Rather unexpectedly, the curves are almost indistinguishable from the corresponding ones, which were measured at much lower Mach numbers of 0.2 and less. A systematic step-by-step variation of M then was undertaken at our reference point $X=3$, $R=0.5$, and for a representative range of St, to check the validity of this important finding (Fig. 5).

Two equally important conclusions may be drawn from Fig. 5. First, the data points lie along almost straight lines. Since the measurements were done on different days under slightly varying running conditions of the jet, this indicates a very high degree of reproducibility over the whole series of experiments.

Second, one may conclude that the structure of the turbulent pressure as expressed by its expansion in azimuthal constituents varies only slightly with M. This information is extremely valuable since it allows us to accept previously obtained correlation results, such as those in Refs. 5 and 6, as also being valid for values of M, which would be more realistic in real jet engines. For the same reason, many of the cross-spectrum measurements still to be done will be performed at just one moderate Mach number of 0.5.

The practically nonexisting effect of M on the percentage of energy contained in the low-order azimuthal constituents does not necessarily imply that $\tilde{p}_\omega$ also is independent of M when suitably normalized by $\rho_0 U_0^2$. Corresponding results at the reference point (Fig. 6) and in the core (Fig. 7) in fact show that M has a considerably stronger effect on the normalized pressure intensity than it ever has on its composition by azimuthal constituents, i.e., on its space-time structure.

The continuous decay of $\tilde{p}/\rho_0 U_0^2$ with M is mainly caused by the frequency components near the spectral peak at $St=0.45$, as may be inferred from the lower part of Figs. 6 and 7. Thus, we may conclude that the main effect of M is on the shape of the spectra, which seem to flatten as M increases.

The considerable decrease in the $St=0.45$ component, according to Fig. 6 for M varying between 0.3 and 0.7, would, of course, also have a stringent effect on $C_{\omega,m}$ and $Q_{\omega,m}$ and, via $\tilde{W}_{12,m}$, on the source integral [Eq. (3)]. We may suggest that the sound prediciton will depend more critically on how W_{p1p2} departs (with M) from the dimensionally logical $(\rho_0 U_0^2)^2$ dependence than on variations of the turbulence structure with M. This is a most favorable result, since it would be a formidable task to repeat all of the pressure source correlations for every M, while it is less troublesome to measure just the pressure intensities and spectra at different Mach numbers.

Characteristics of Pressure Cross-Spectra

The foregoing discussion of the jet pressure field was in terms of its intensity, spectra, and composition by azimuthal constituents. The dominance of the low-order (small m) constituents is a manifestation of high statistical coherence of narrowband signals detected at circumferentially displaced positions ($\Delta\phi$). Some earlier longitudinal (ΔX) and lateral (ΔR) correlation measurements[6] have revealed that those frequency components that are well-correlated circumferentially also exhibit strong axial and radial coherence.

Thanks to our recent computer analysis, we are able now to evaluate more general cross-correlations with the fixed probe at several axial positions and the moving probe being displaced axially, radially, and circumferentially. Only a few of these results will be reported here, with our reference point ($X=3$; $R=0.5$) chosen for the fixed probe. They will be given in the form of coherence functions

$$\frac{S_\omega}{\tilde{p}_{\omega,1}\tilde{p}_{\omega,2}}=\frac{(C_\omega^2+Q_\omega^2)^{1/2}}{\tilde{p}_{\omega,1}\tilde{p}_{\omega,2}} \tag{19}$$

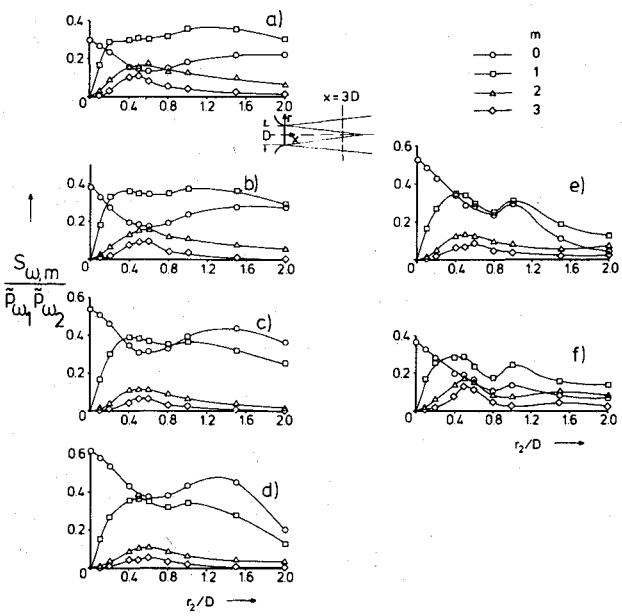

Fig. 8 Constituents of normalized radial coherence of pressure in plane: $x_1=x_2=3D$. $D=5$ cm; $M=0.5$; fixed probe at $r_1=0.5D$; St, see legend of Fig. 3.

$$\frac{S_{\omega,m}}{\tilde{p}_{\omega,1}\tilde{p}_{\omega,2}}=\frac{(C_{\omega,m}^2+Q_{\omega,m}^2)^{1/2}}{\tilde{p}_{\omega,1}\tilde{p}_{\omega,2}} \tag{20}$$

These, together with the phase angle $\Psi_{\omega,m}=\arctan Q_{\omega,m}/C_{\omega,m}$ and the corresponding intensity distribution of the pressure contain all of the information we need to evaluate the source integral [Eq. (3)].

Figure 8 shows typical radial coherence of the $m=0$, 1, 2, 3 constituents for our standard set of Strouhal numbers. All but one curve ($m=0$) drop to zero at $R_2=0$. This must be so, since all but the axisymmetric pressure constituent vanish on the axis of symmetry of the jet. The coherence of the $m=0$ and $m=1$ constituents is particularly strong for radii between one and two jet diameters from the axis, i.e., where the mean flow quantities have already dropped to zero. It is not quite clear how the curves would behave for $R_2>2$. This question, however, is not relevant for two reasons. First, $\tilde{F}_{r,m}$ would limit the extent of the relevant source region in the way discussed previously. Second, it is not the normalized cross-spectrum that counts in the sound generation process, but its absolute values. Multiplication by the local values of $\tilde{p}_\omega$ would already change the curves in Fig. 8, as may be seen from the distribution of $\tilde{p}_\omega$ ($St=0.45$) over R_2 depicted in Fig. 9.

The unresolved coherence $S_\omega/\tilde{p}_{\omega 1}\tilde{p}_{\omega 2}$ does not drop monotonically with the probe displacement as one might expect, but shows a minimum around $R=0.8$, i.e., at the fringes of the mixing region where the turbulence is known to be highly intermittent in character (compare the lower graph of Fig. 9). A comparison with the $St=0.45$ plot on Fig. 8

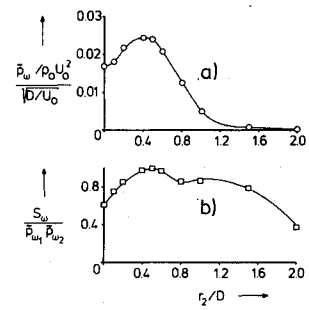

Fig. 9 Radial variation of normalized pressure spectral density a) and radial coherence, b) in plane $x_1=x_2=3D$; $\Delta\phi=0$; $D=5$ cm; $M=0.5$; fixed probe at $r_1=0.5D$; $St=0.45$.

shows that this coherence defect near $R_2 = 0.8$ with a subsequent maximum near $R_2 = 1.2$ is entirely due to a corresponding behavior of the $m = 0$ and 1 constituents; the coherence of the axisymmetric pressure constituent definitely is highest when the moving probe is well outside the mixing region. The situation is different for $m = 2$ and 3, and, presumably, for the higher-order constituents.

The result of cross-correlations for axial and circumferential probe displacements is presented in Fig. 10. With both probes in the central mixing region, the coherence distributions show no anomalies. The decay of coherence with X is strongest for frequencies on both sides of the spectral peak which, for our reference point, $X_1 = 3$, is at $St = 0.45$. The $St = 0.45$ component is seen (Fig. 11) to reach its maximum intensity at $X = 3$.

Although for $St = 0.45$, S_ω and its $m = 0$ and 1 constituents decay almost symmetrically with positive and negative displacements ΔX, this is not the case for the higher frequencies in Fig. 10. Knowing that the higher frequency components reach their maxima nearer to the jet exit (compare Fig. 8 of Ref. 5), one might suggest that symmetric coherence curves are obtained when the fixed probe is positioned at the axial distance where the St-component under consideration reaches its maximum.

Comparison of Results with Direct Source Identifications

The last statement reflects the generally accepted view that different axial segments of the jet are responsible for different frequency components being generated. In this context, the results of Seiner and Reethof[10] are of special interest. Their source coherency results obtained by a direct correlation between far-field and near-field fluctuations (cf., their Figs. 14 and 16) clearly show that the shear noise generation process may be attributed to jet source regions which lie further downstream as the frequency becomes lower. Their shear noise coherency for Strouhal components between 0.2 and 1.5 peaks at almost exactly those axial positions where the fluctuating flow pressure reaches a maximum in the mixing region. Figure 12 compares the position of maximum pressure intensity with the conjectured position of maximum shear noise emission (from Fig. 16 of Ref. 10).

Seiner and Reethof[10] also concluded that the shear noise dominates the self-noise by at least a factor of 10 dB for a radiation angle $\Theta = 30°$ to the jet axis. This lends support to

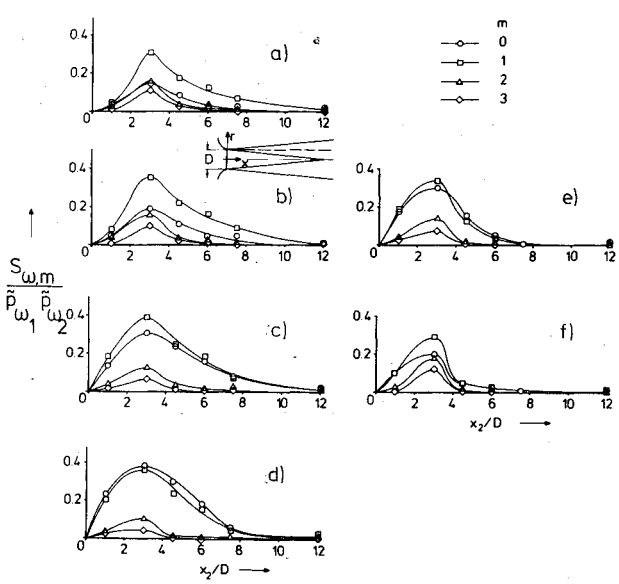

Fig. 10 Constituents of normalized axial coherence of pressure in central mixing region $r_1 = r_2 = 0.5D$. $D = 5$ cm; $M = 0.5$; fixed probe at $x_1 = 3D$; St, see legend of Fig. 3.

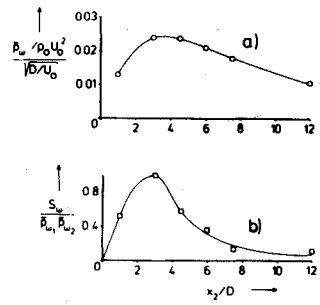

Fig. 11 Axial variation of normalized pressure spectral density a) and axial coherence b) in central mixing region $r_1 = r_2 = 0.5D$; $\Delta\phi = 0$; $D = 5$ cm; $M = 0.5$; fixed probe at $x_1 3D$; $St = 0.45$.

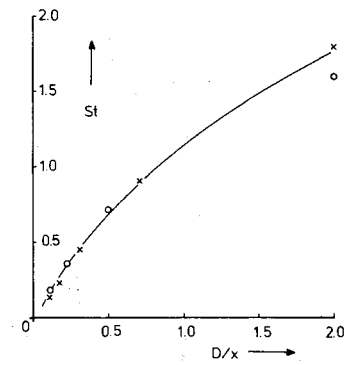

Fig. 12 Axial positions in a circular jet where a given Strouhal component reaches its maximum intensity: × turbulent pressure measurements in central mixing region $r = 0.5D$ (from Ref. 5, Fig. 8); o shear noise source coherency measurements under $\Theta = 30°$ to jet axis (from Ref. 10, Fig. 16).

our own source model, which neglects the nonlinear source terms.

Hurdle, Meecham, and Hodder,[11] who correlated the far-field pressure directly with the jet flow pressure in a real jet engine, are in general agreement with the results of Ref. 10. Both investigations show highest source-sound coherences of up to more than 10% for $\Theta = 30$ deg and the flow probe closer to the jet axis and near the tip of the potential cone. Since only the axisymmetric ($m = 0$) source constituent can exist on the axis, this is an indication that there must also exist a strong $m = 0$ component in the radiated noise. This does not mean, as suggested by the authors, that the sound region is confined near the jet axis. It does, however, tell us that the other azimuthal constituents of the source field which contribute to the intensity at off-axis positions are less efficient in generating sound. Hence, these components reduce the measured source coherency for source points at $R = 0.5$, although here the $m = 0$ constituent may well be stronger than at $R = 0$.

Probably the strongest support for the importance of coherent structures with respect to jet noise and for the model proposed in the present paper comes from a paper by Dahan and Elias.[12] With the aid of a reference signal from an infrared radiation detector, these authors were able to determine the coherency between the near-field and far-field pressure fluctuations with any probe/flow interference thus being excluded. They found particularly high normalized coherence values up to 0.5 in the relevant range $0.1 < St < 1$ with the far-field microphone at small angles ($\Theta = 20$ deg) in striking contrast to an almost neglibible coherency for far-field angles of 90 deg to the axis.

Conclusions

We now may conclude that for Strouhal numbers between 0.1 and 1 the turbulent jet pressure field exhibits a pronounced peak in its spectrum, and a particularly strong coherence in the source region. The coherency measurements of Refs. 10-12 seem to indicate that the coherent turbulence structures predominantly radiate at small angles Θ. This,

however, is exactly that range of parameters in which one expects the mean flow/turbulence interactions to play an important role in the sound generation mechanism. Our theory, as reviewed previously, thus would appear to be appropriate for a quantitative prediction of the sound at low or moderate *St* radiated at angles 0 deg$<\Theta<$45 deg, where the maximum of the directivity pattern is known to occur.

This view contradicts the widespread philosophy that the nonlinear turbulence/turbulence interactions act as the primary sources of noise, and that the sheared mean flow has a secondary shrouding effect on the sound waves, which are thought of as emanating from small-scale turbulent elements (eddies). By using the previously described pressure characteristics in a numerical evaluation of the source integral [Eq. (3)], it might be possible to decide which model is more realistic in the range of parameters indicated.

Acknowledgments

We would like to thank our colleagues at the DFVLR: U. Michel for writing the computer programs and W. F. King for his assistance in proofreading the manuscript.

References

[1] Fisher, M. J. and Lowson, M. V., "Aerodynamic Noise," *Journal of Fluid Mechanics*, Vol. 48, 1971, pp. 593-603.

[2] Ffowcs-Williams, J. E., "Technical Evaluation Report on Fluid Dynamics Panel Specialists Meeting on Noise Mechanisms," AGARD-AR-66, 1974.

[3] Davies, P.O.A.L. and Yule, A. L., "Coherent Structures in Turbulence," *Journal of Fluid Mechanics*, Vol. 69, 1975, pp. 513-537.

[4] Michalke, A., "An Expansion Scheme for the Noise from Circular Jets," *Zeitschrift für Flugwissenschaften*, Vol. 20, 1972, pp. 229-237.

[5] Michalke, A. and Fuchs, H. V., "On Turbulence and Noise of an Axisymmetric Shear Flow," *Journal of Fluid Mechanics*, Vol. 70, 1975, pp. 179-205.

[6] Fuchs, H. V., "Space Correlations of the Fluctuating Pressure in Subsonic Turbulent Jets," *Journal of Sound and Vibration*, Vol. 23, 1972, pp. 77-99.

[7] Fuchs, H. V., "Measurement of Pressure Fluctuations within Subsonic Turbulent Jets," *Journal of Sound and Vibration*, Vol. 22, 1972, pp. 361-378.

[8] Lau, J. C., "The Coherent Structure of Jets," University of Southampton, Ph.D. Thesis, 1971.

[9] Bradbury, L. J. S. and Khadem, A. H., "The Distortion of a Jet by Tabs," *Journal of Fluid Mechanics*, Vol. 70, 1975, pp. 801-813.

[10] Seiner, J. M. and Reethof, G., "On the Distribution of Source Coherency in Subsonic Jets," AIAA Paper No. 74-4, Washington, D.C., 1974.

[11] Hurdle, P. M., Meecham, W. C., and Hodder, B. K., "Investigation of the Aerodynamic Noise Generating Region of a Jet Engine by Means of the Simple Source Fluid Dilatation Model," *Journal of the Acoustical Society of America*, Vol. 56, 1974, pp. 1708-1721.

[12] Dahan, C. and Elias, G., "Source Structure Pattern in a Hot Jet by Infrared-Microphones Correlations," AIAA Paper No. 76-542, Palo Alto, Calif., 1976.